Nuclear Engineering and Technology 57 (2025) 103617

Contents lists available at ScienceDirect

Nuclear Engineering and Technology

journal homepage: www.elsevier.com/locate/net

Original Article

Enhancing the shape memory performance of self-reinforced cross-linked polyethylene composites by the optimization of the production temperature

Balázs Tatár [a], Renáta Homlok [b], László Mészáros [a,c,*]

[a] Department of Polymer Engineering, Faculty of Mechanical Engineering, Budapest University of Technology and Economics, Műegyetem rkp.3, H-1111, Budapest, Hungary
[b] Radiation Chemistry Group, Surface Chemistry and Catalysis Department, Institute for Energy Security and Environmental Safety, HUN-REN Centre for Energy Research, Konkoly-Thege M. street 29-33, H-1121, Budapest, Hungary
[c] HUN-REN Research Group for Composite Science and Technology, H-1111 Műegyetem rkp.3, H-1111, Budapest, Hungary

ARTICLE INFO

Keywords:
Shape memory polymer
Self-reinforced composite
Film stacking
Cross-linked polyethylene
Mechanical testing

ABSTRACT

In this study, we investigated the shape memory properties of ionizing radiation cross-linked high-density polyethylene (HDPE) self-reinforced by Dyneema fibers. We investigated self-reinforcement as a means of increasing the recovery stress (σ_{rec}), which has not been extensively researched before in the literature. Using film stacking, we produced composites with effective self-reinforcement and samples where the fibers were completely melted by high temperatures as reference samples. The composites were cross-linked by gamma irradiation with a 150 kGy dose, and we verified the cross-linked state with swelling tests. We characterized the self-reinforced composites through differential scanning calorimetry (DSC), scanning electron microscopy (SEM), and flexural tests. We found the optimal processing temperature to be 150 °C, where the fibers remained intact, but adhesion was excellent. Self-reinforcement slightly decreased the recovery ratio (R_r), at the same time, it increased σ_{rec} of the samples by 111 %, as it increased the programming stress. We investigated different programming temperatures and found that higher temperatures produced higher R_r but lower σ_{rec}. We showed that through self-reinforcement we can manufacture all-polymer composites with increased σ_{rec}. All polymer composites can be fully biodegradable, biocompatible, and have lower density than conventional composites, which properties can be advantageous in future applications.

1. Introduction

Shape memory polymers (SMPs) are intelligent materials capable of altering their shape in response to an external, non-mechanical stimulus. They can be programmed to respond to a wide range of stimuli, the most common being heat [1]. Shrink tubes and shrink packaging already make use of this technology [2], but other fields can also profit from it, such as 4D printing, biomedicine, robotics, and control technology [3–7].

The shape memory effect in polymers is based on a dual structure, where the polymer possesses so-called switches and netpoints. The roles of switches and netpoints can be played by many different structures, like phases or chemical bonds. Switches have to transition from an "open" state that enables molecular movement to a "closed" one that restricts it in response to the stimulus, while netpoints have to remain in place, holding the material together throughout [8,9].

One of the most widely applied SMPs is cross-linked polyethylene (X-PE), where the primary chemical bonds are the netpoints and the crystalline phase is the switch. The shape memory effect in X-PE occurs on the crystalline melting temperature (T_m) if the material has been programmed to respond. Thus, to complete a shape memory cycle, we have to heat the polymer above its T_m, to open the switches via crystalline melting. In this easy-to-deform state, we have to apply strain on the sample and deform it to the programmed shape. During this step, the netpoints maintain the material's integrity, and internal stress is stored in the structure. We should keep this deformed state until the material is cooled down and crystallized so the switches close. When the external force is removed, some of the strain may relax. Subsequently, when the material is heated above the T_m the switches release again, causing the stored stress to be released and the sample to be returned to its original shape, potentially leaving some residual strain [9–11].

During the shape memory cycle, the SMP stores and releases stress.

* Corresponding author. HUN-REN Research Group for Composite Science and Technology, H-1111, Műegyetem rkp.3, H-1111, Budapest, Hungary.
E-mail address: meszaros@pt.bme.hu (L. Mészáros).

https://doi.org/10.1016/j.net.2025.103617
Received 21 December 2024; Received in revised form 13 March 2025; Accepted 30 March 2025
Available online 1 April 2025

This stress determines the ability of the SMP to recover while under a constraint or external force or to move other objects while recovering. The strength of the recovery can be measured by the recovery stress (σ_{rec}). Polymers usually exhibit much lower σ_{rec} than shape memory alloys; thus, their use is limited in applications where recovery under load is required [9,10,12].

Recovery stress can be increased by composite reinforcement, which increases the stress required to deform the material, so the SMP can store more stress and release more stress. Both fiber and nanoparticle reinforcement are common research topics [12–14].

Shape memory polyethylene (PE) has already been reinforced with different fibers and nanoparticles [15]. For PE to have shape memory properties, it has to be cross-linked, usually by 50–250 kGy absorbed dose of ionizing irradiation [16], but the absorbed dose required for cross-linking and the properties of X-PE are highly dependent on the parameters of the irradiation and the composition of the material [17]. Wang et al. [16,18] investigated the effects of short glass fibers on cross-linked poly (styrene-b-butadiene-b-styrene) (SBS) triblock copolymer/X-PE blends. The inclusion of glass fibers resulted in a slower recovery process. However, the precision of recovery increased in cyclical tests, which they explained with a decrease in plastic deformation. Wang et al. [19] also investigated short carbon fiber reinforcement, which led to slower recovery, like glass fibers. Unlike the glass fibers, they also decreased the recovery ratio (R_r), which the authors explained with a decreased percentage of the material taking part in shape memory. Rezanejad and Kokabi [20] added nanoclay particles to the X-PE matrix. The presence of nanoclay resulted in increased σ_{rec} while R_r decreased, which the authors explained with a reduction in molecular mobility. Ma et al. [21] used carbon black to reinforce a two-way shape memory X-PE and found that it slightly decreased the accuracy of the shape memory but increased the strength of the material. Zhang et al. [22] conducted shape memory experiments on an ultra-high molecular weight polyethylene (UHMWPE)/PE blend reinforced with carbon nanotubes. They found that the reinforcement slightly increased the R_r, but the authors did not investigate the mechanical characteristics. Reinforcement of X-PE can increase σ_{rec} but often reduces the precision of the recovery.

In the case of PE, self-reinforced polymer composites (SRPCs) can sometimes offer a better reinforcing method than conventional composites. SRPCs have a lower density than conventional composites; they offer better adhesion between fibers and matrix, and their recycling can be easier [23]. Self-reinforcement can also possibly take part in shape memory, boosting its effectiveness. UHMWPE, is an exceptionally strong type of PE [24], fibers made out of it have strength and modulus comparable to conventional fibers [25]. Thus, they are available as a convenient reinforcing material [26–28].

There has already been substantial research into self-reinforced PE with UHMWPE fiber reinforcement [29]. Film stacking is a production method where matrix sheets or films and fiber layers are alternated and compression molded to make samples [30]. This technology is well suited to making PE-based SRPCs with a wide range of possible fiber contents, where the reinforcement increases the strength and modulus of the material [31–33] For the highest strength, the melting and recrystallization of the fibers should be avoided during processing while achieving good adhesion with the matrix. For UHWMPE fibers, the optimal processing temperature is between 140 and 150 °C [31,34].

However, very little research has been conducted into the shape memory characteristics of the self-reinforced PE composites [35]. Closest to it is the shape memory of PE fibers, utilized in artificial muscles, where the high strength and shape memory of UHMWPE fibers are exploited [36–38]. Maksimkin et al. [39] examined the shape memory behavior of UHMWPE fibers. Although the polymer lacks chemical cross-links, its high molecular weight allows the entanglement of amorphous chains to act as the netpoints, while the crystalline domains can act as the switches. The researchers compared these findings with UHMWPE in its bulk state, which also displayed shape memory due to similar mechanisms. Notably, UHMWPE fibers exhibited significantly greater recovery stress when compared to the bulk samples.

In this research, we investigated the shape memory characteristics of self-reinforced PE composites produced by films stacking from UHWPE fibers and high-density polyethylene (HDPE) matrix which have not been extensively researched before in the literature. Our aim was to increase the recovery stress (σ_{rec}). A shape memory SRPC can be fully biocompatible and have a lower density than conventional composites. We compared the effect of self-reinforcement to samples where the fibers have been completely melted and mixed with the matrix. Based on the findings of Amer and Ganapahiraju [31], we achieved this by raising the production temperature above the T_m of the fibers, so any effect resulting from an increased molecular weight or any other factor could be negated. For this reason, we produced samples at a wide range of production temperatures, from 130 °C to 160 °C, to find the optimal temperature and to also obtain samples with negated self-reinforcement. We theorized that optimal temperature self-reinforcement would increase the recovery stress compared to samples produced at high temperatures. We used gamma irradiation to cross-link the samples to give them shape memory properties. We then characterized the morphology of these samples and investigated both free and constrained recovery.

2. Materials and methods

2.1. Materials used

As a matrix for the SRPCs, we used TIPELIN BA 550-13 high-density polyethylene (HDPE) manufactured by MOLGroup Chemicals, Hungary. The matrix was reinforced with Dyneema SK76-type UHWMPE fibers sourced from Koninklijke DSM N. V., Netherlands.

2.2. Production of SRPCs

The manufacturing process of composites is shown in Fig. 1.We applied the film stacking method to produce the composites. As a first step in the production process for each sample, we compression molded 3 pieces of 160 × 160 × 0.5 mm sheets from the matrix material on a Teach-Line Platen Press 200 E (Dr. Collin GmbH, Germany) at 160 °C with 7 bar pressure. We held the temperature for 10 min before compressing, and cooled the sheets in the press while keeping up the pressure, by circulating water through the pressing plates until they reached room temperature. Subsequently, we used a custom-made coiler machine to wrap 20 wt% of Dyneema fibers around one of the sheets. We then placed this sheet between two other 0.5 mm thick sheets and compressed them on the same machine at 7 bar pressure to produce 160 × 160 × 2 mm SRPC sheets. At this step, different temperatures were used to produce different samples. The applied temperatures were 130, 135, 140, 145, 150, 155 and 160 °C.

Finally, we cross-linked the composites to achieve shape memory properties. We sealed one sheet produced at each temperature in PE bags and irradiated them with a dose of 150 kGy. Institute of Isotopes Ltd. (Budapest, Hungary) conducted the irradiation with a panoramic SLL-01 ^{60}Co radiation source, with a steady irradiation rate of 2 kGy/h. We cut the specimens from the sheets with a precision saw.

2.3. Characterization methods

2.3.1. Differential scanning calorimetry (DSC)

We conducted DSC measurements to investigate the crystalline properties of the samples using a TA Instruments Q2000 DSC (TA Instruments, USA). We cut 5–7 mg samples and tested them between 40 and 180 °C in a heat-cool-heat cycle. The heating rate was 5 °C/min for both heating and cooling. We conducted the tests in an N_2 atmosphere with a 50 ml/min flow rate. As the degree of crystallinity depended highly on the content of fibers in the DSC sample, and fiber pullout was impossible to avoid in DSC sample preparation, we weren't able to

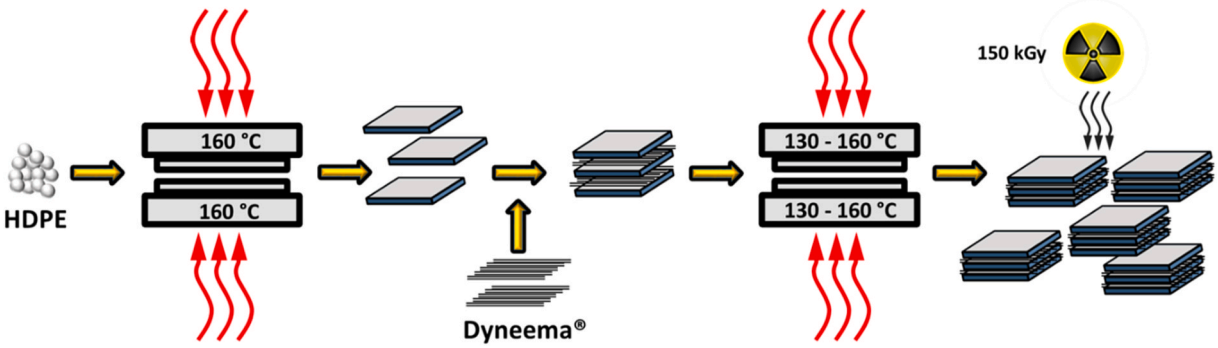

Fig. 1. The manufacturing process of self-reinforced shape-memory composites.

calculate the precise degrees of crystallinity for the sheets [40].

2.3.2. Swelling experiments

The swelling characteristics of the samples correspond to the degree of cross-linking. For this reason, we swelled and weighed the irradiated and un-irradiated samples to confirm that cross-linking occurred and compare cross-linking between samples. Two approximately 1 g specimens were cut out from each sample, weighed precisely, and swelled in xylene at room temperature for 72 h. After swelling, we wiped the specimens with paper and weighed them again. We tested 5 specimens for each sample and calculated the swelling ratio as the average ratio of the mass after and before swelling.

2.3.3. Scanning electron microscopy (SEM)

To observe the presence or lack of visible fibers directly, as well as the adhesion between fiber and matrix and the layers in the composite, we took scanning electron microscope (SEM) images of the cut surfaces of the samples. Cutting the samples was necessary due to their toughness, as they didn't fully break under liquid nitrogen. The cut surfaces do not represent the original morphology, but their comparison still reveals much about the properties. We used a JEOL JSM 6380LA (Jeol Ltd., Japan) machine, before inspecting them, we sputtered the samples with a thin gold layer.

2.3.4. Flexural tests

We conducted flexural tests on 40 × 25 × 2 mm specimens cut from the sheets in the direction of the fiber orientation to assess the mechanical properties at room temperature. We tested five specimens of each sample on a Zwick Z005 universal testing machine (Zwick GmbH., Ulm, Germany) with a 5 kN cell. The test speed was 20 mm/s, and the span between supports was 32 mm. The tests lasted until the specimen broke or reached the conventional deflection, 10 % of the span, which was 3.2 mm. We calculated the flexural modulus as the slope of the tangent at the initial near-straight part of the bending curve.

2.3.5. Free- and constrained recovery experiments

We evaluated the precision of the shape recovery of the samples in free recovery experiments and the recovery stress in constrained recovery experiments. We conducted both with the same Zwick Z0250 universal testing machine (Zwick GmbH., Ulm, Germany) equipped with a 1 kN cell and a heating chamber. We put the 40 × 25 × 2 mm samples in a 3-point bending head with a 32 mm span between supports. The samples were heated in the heating chamber at 130 °C for 5 min, deformed to a 2 mm deflection (ε_m). Keeping the crosshead in place, they were removed from the heating chamber and cooled at room temperature for 5 min. Subsequently, we put them back into the heating chamber for 5 min while recovery took place (Fig. 2). We tested 3 specimens of each sample.

In the case of the free recovery experiments, the deformations were precisely monitored using a Mercury Monet (Sobriety, Czech Republic) type digital image correlation (DIC) device. The deflection was monitored using a single-point probe in the middle of the specimen. We calculated the shape recovery ratio using Equation (1) from the deflection data.

$$R_r = \frac{\varepsilon_m - \varepsilon_p}{\varepsilon_m}\ [-] \tag{1}$$

where ε_m is the maximum strain applied, and ε_p is the persisting strain after recovery [41].

In the case of constrained recovery cycles, we kept a constant deflection of 0.01 mm in place during recovery and monitored the force on the crosshead with the cell. We then calculated σ_{rec} from the maximum force. For the constrained recovery experiments, we also measured the stress required to deform the specimen to the programmed shape, the programming stress (σ_{prog}). We calculated the storage ratio (S) using Equation (2) to characterize the material's ability to store and release the programming stress:

$$S = \frac{\sigma_{prog}}{\sigma_{rec}}\ [-] \tag{2}$$

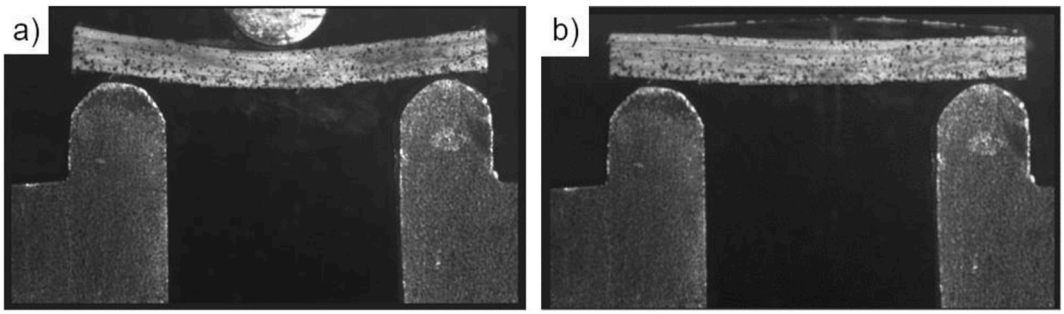

Fig. 2. The DIC images of the shape memory experiments: the deformed shape (a) the recovered shape (b).

3. Results and discussion

3.1. Swelling experiments

While different production temperatures affected the swelling rate of the samples (Fig. 3), it is clear that, on average, unirradiated samples swelled more than irradiated ones. Below 145 °C, the composites were poorly impregnated and had varying porosities (also supported by the SEM images), which impacted the results more than the irradiation. High porosity also made the samples have a high degree of swelling, and indicates weaker bonding between the fibers and matrix. Above this temperature, the adhesion improved, and the process stabilized. The irradiated samples above 145 °C had lower swelling, showing that the absorbed dose was sufficient to cross-link the samples.

3.2. DSC experiments

DSC measurements on unirradiated samples revealed that at low temperatures, the fibers remained separate from the matrix, and the composite produced two distinct peaks Fig. 4. The peaks around 145–150 °C belonged to the Dyneema fibers, which had parallel molecules in a highly crystalline structure, while the peaks around 135 °C belonged to the folded chains of the HDPE matrix [42,43]. At higher temperatures, the peak for the Dyneema fibers disappeared, and only the lower temperature peak showed, indicating that at these temperatures, the fibers melted, and no effective reinforcement took place. The UHMWPE of the fibers recrystallized in the same way as the HDPE from the matrix. There was no significant difference between the degrees of crystallinity or the melting temperatures.

3.3. Scanning electron microscopy

Despite the careful preparation, we could not cut the 130 °C and 135 °C samples without the complete delamination of the composite. Thus, SEM images for these are not available. The delamination during sample preparation occurred because of the poor adhesion between the fibers and matrix, as the matrix did not melt properly during production. Regarding the prepared samples (Fig. 5), when the production temperature was 155 °C and 160 °C (Fig. 5/d,e), we could not see fibers in the samples, as shown also in the DSC experiments at these temperatures, the fibers melted. For the samples where fibers are present (Fig. 5/a,b,c), we can see that the fibers remained in distinct layers and did not mix evenly into the matrix. For the 150 °C sample (Fig. 5/c), the fiber layers split apart less than for the samples produced at lower temperatures, which indicates that the matrix stuck to the fibers, and penetrated the

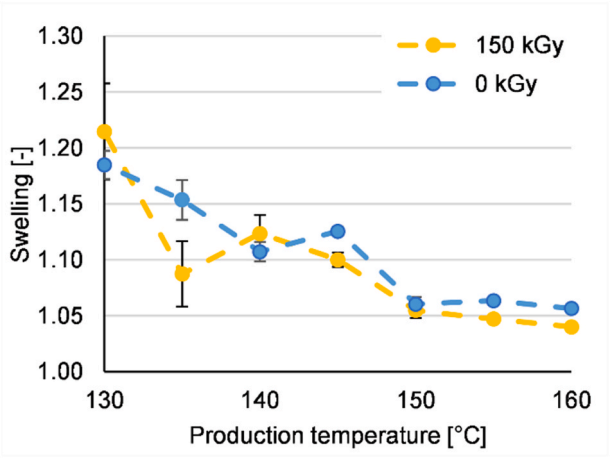

Fig. 3. Swelling rates of irradiated and unirradiated samples produced at different temperatures.

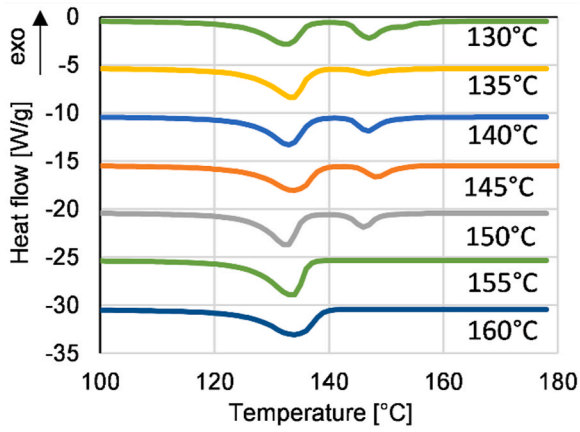

Fig. 4. DSC curves of unirradiated samples produced at different temperatures (given below the curves).

layers more which is important for high strength and modulus. Here, we can also see that the fibers appear slightly thinner, likely from partial melting and some relaxation could also have occurred. The amount of fibers observed on each image is likely a result of sample preparation and does not indicate an overall change in the fiber content of the samples.

3.4. Flexural tests

The flexural tests showed an optimal production temperature for both the maximal stress and modulus in the investigated temperature range (Fig. 6). However, these did not coincide precisely; in the case of the unirradiated samples, the 140 °C produced the highest average flexural strength, while the standard deviations of 140 °C, 145 °C and 150 °C overlapped. In the case of the irradiated samples, the maximum flexural strength was clearly 150 °C (Fig. 6/a), while in terms of modulus, the maximum was achieved at 145 °C (Fig. 6/b). In conclusion, we can say that a production temperature of 145 °C–150 °C produced the highest strength composites. Below this temperature, the poor adhesion of the fibers and matrix limited the strength of the composite, particularly at 130 °C, while above this temperature, the melting of the fibers drastically reduced the strength of the composite. There was negligible change between 155 °C and 160 °C, so we can say that for both, the fibers melted, and we can take them as references for an unreinforced sample. Composites with higher strength and modulus can have increased recovery stress during shape memory.

As a result of the irradiation, the strength and modulus of the composites increased. The irradiation caused the PE to cross-link, and cross-linked polyethylene has a higher strength than the virgin material [44]. The increase is most pronounced in the case of the 145 and 150 °C samples, where because of the good adhesion between the matrix and fibers, the irradiation could result in covalent bonds between the two.

3.5. Free recovery experiments

In the free recovery tests, all samples demonstrated shape-memory properties, although under 150 °C, the recovery was imprecise (Fig. 7/a). The recovery ratio was 68 % for samples produced at 130 °C. In this sample, the fibers likely played a very small part in the process, as the adhesion between them and the matrix was very poor. When the production temperature increased, for 135 °C and 140 °C samples, the recovery ratio decreased to around 55 %. The reduction likely resulted from the fibers now connecting to the matrix but not being encompassed by it, leading to delamination mid-process. With a further increase in temperature up to 150 °C, the recovery ratio increased to 82 %, which is considered adequate. The connection between the fibers and the matrix

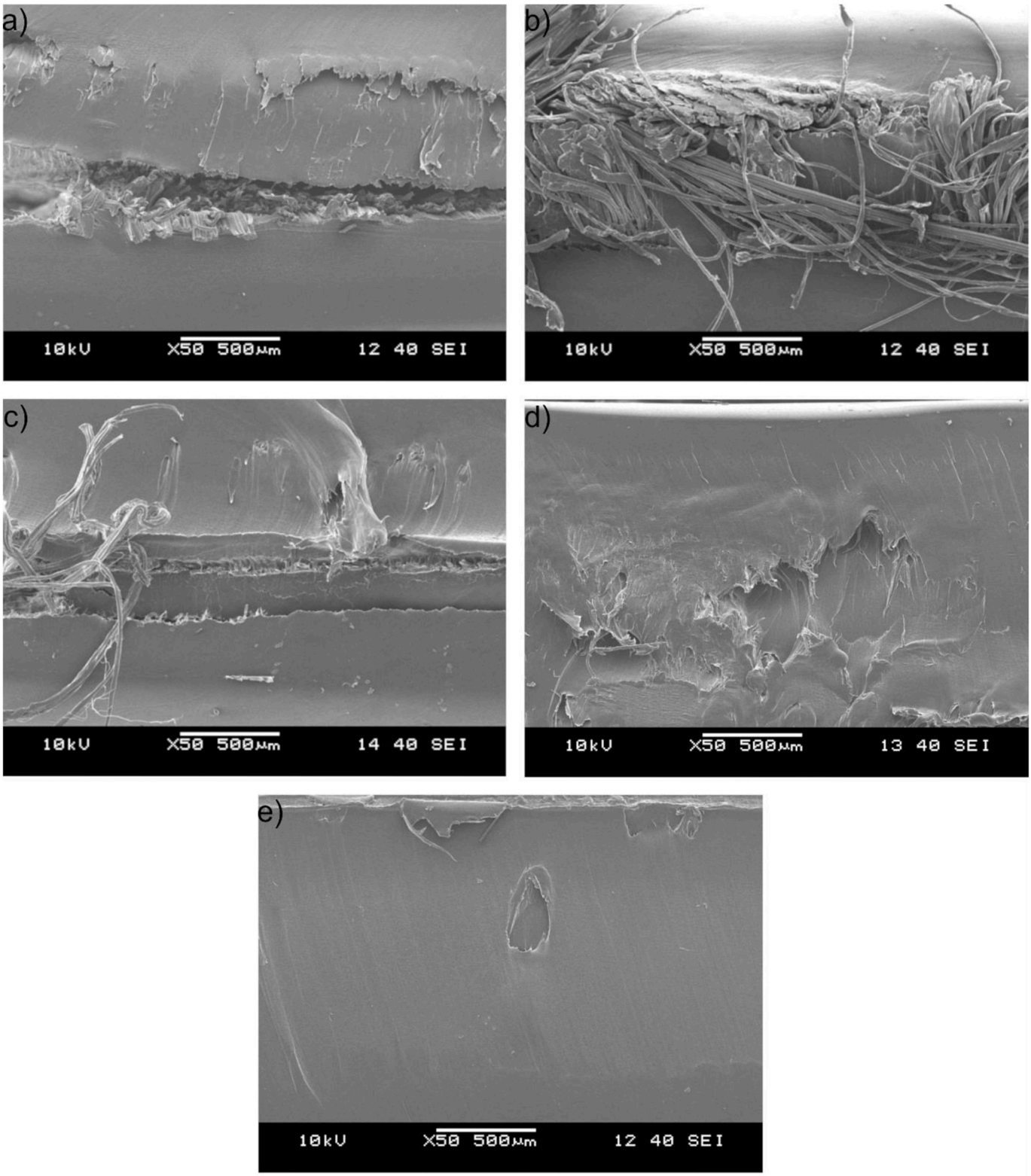

Fig. 5. SEM images of the cut surfaces of unirradiated samples produced at 140 °C a), 145 °C b), 150 °C c), 155 °C d), 160 °C e).

improved, leading to a reduction in irrecoverable deformation. Increasing the production temperature to 155 °C and 160 °C led to the complete melting of the fibers, which negated any negative effects from fiber reinforcement, leading to an increase in the recovery ratio, although only with the standard deviations overlapping. The large standard deviation at 150 °C resulted from the partial melting of the fibers.

When we varied the transition temperature for samples produced at 145 °C, we could see a positive correlation between the transition temperature and the recovery ratio (Fig. 7/b). There were small increases up to 150 °C, from more thorough melting, and a significant increase at 160 °C resulting from the complete melting of the same effect that we have seen at 155 and 160 °C in Fig. 7/a.

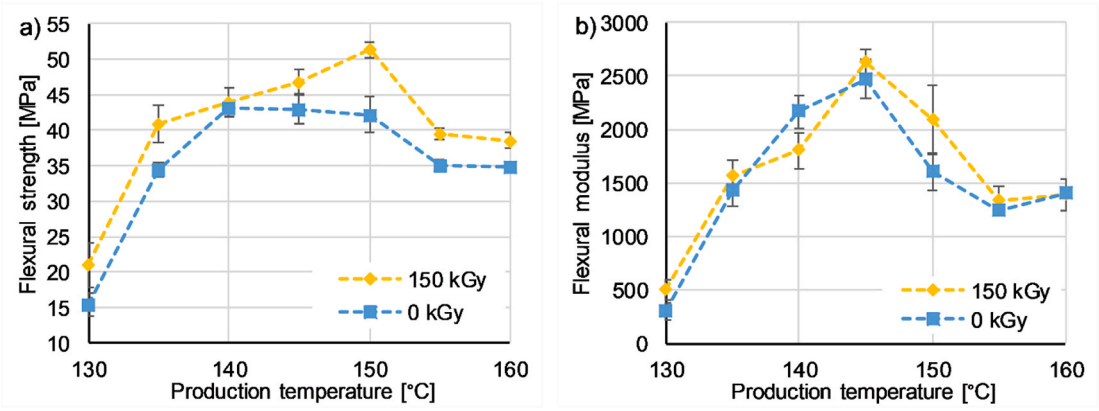

Fig. 6. Flexural stress a) and flexural modulus b) of irradiated and unirradiated samples produced at different temperatures.

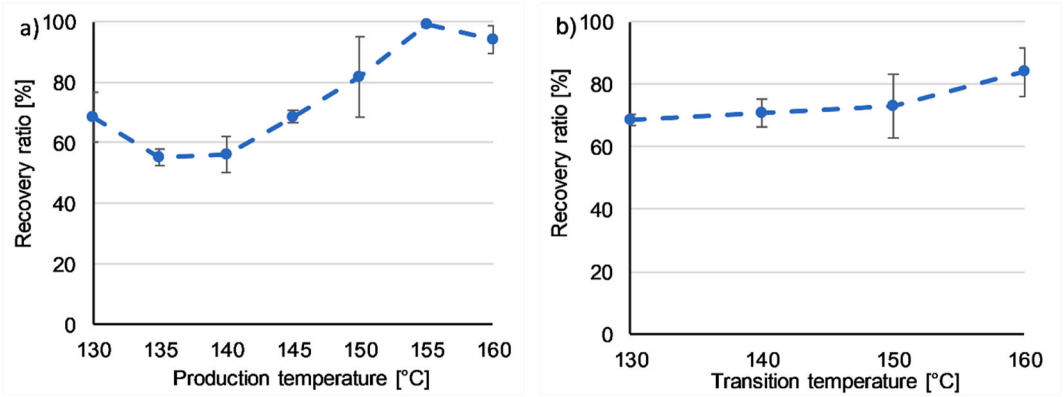

Fig. 7. Recovery ratios of irradiated samples produced at different temperatures a) and recovery ratios of irradiated samples produced at 145 °C programmed and recovered at different temperatures b).

3.6. *Constrained recovery experiments*

Based on the constrained recovery experiments, we can conclude that effective fiber reinforcement could increased the recovery stress of the samples compared to the samples produced at high temperatures (Fig. 8/a). The recovery stress and programming stress results of the samples correlated with the flexural strength at room temperature, as the programming strength is essentially the flexural strength at high temperature. The sample produced at 130 °C performed very poorly because of the poor adhesion between the fibers and the matrix, while the samples produced at 155 °C and 160 °C exhibited low stresses because the fibers were completely melted and could offer little resistance. The samples produced at 135 °C, 140 °C, 145 °C and 150 °C had intact fibers connecting to the matrix and showed similar recovery stresses, with 150 °C showing a clear maximum of 1.7 MPa, outside the standard deviation, which is more than twice that of the high-temperature samples. The high-temperature samples showed the best ability to store the programming stress, but the low programming stress led to low recovery stresses. The 150 °C sample both had an increased programming stress and increased storage ratio, resulting from the partial melting of the fiber surface and good connection.

Increasing the transition temperature for the samples produced at

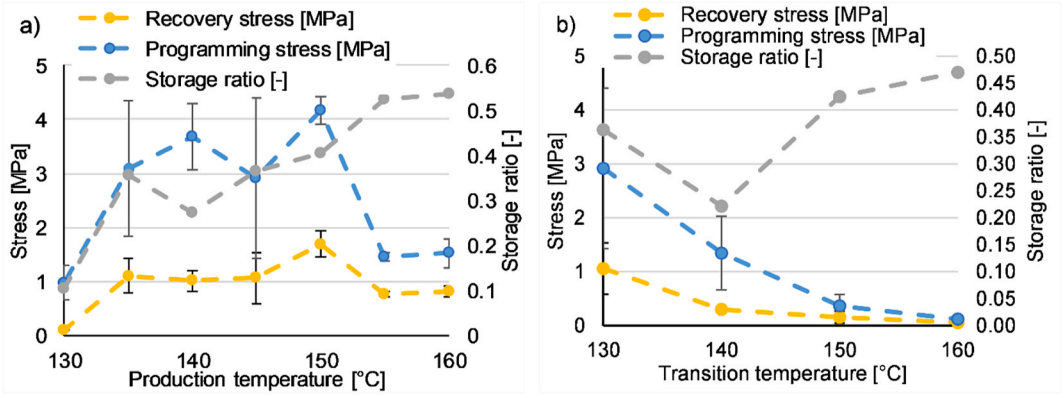

Fig. 8. Constrained recovery characteristics of irradiated samples produced at different temperatures a) and constrained recovery characteristics of irradiated samples produced at 145 °C programmed and recovered at different temperatures b).

145 °C led to decreased programming and recovery stress. As the crystalline phase completely melted, the cross-links alone were not enough to build substantial stress in the material, and thus, the stress could not be stored and recovered properly.

4. Conclusions

We investigated the effect of self-reinforcement on the shape memory of X-PE. By varying the production temperature of film stacking, we produced composites with low adhesion at low temperatures, effective self-reinforcement at the optimum temperatures of 145–150 °C, and samples where the fibers completely melted at high temperatures.

Effective self-reinforcement increased both the flexural strength and modulus of the samples while it slightly decreased the recovery ratio of shape memory, likely resulting from increased plastic deformation. Self-reinforcement increased the recovery stress of the samples, as it increased the stress required for programming while only slightly decreasing the capacity for stress storage. Overall, the high-temperature samples had a higher recovery ratio, while the optimally produced composites had a higher recovery stress. In conclusion, in the case of free recovery, with no impediments, self-reinforcement doesn't improve the shape memory properties. However, if external forces constrain the recovery, the reinforcement increases the load-bearing capacity of the polymer, improving the shape memory effect.

We investigated the effect of different programming temperatures on the shape memory characteristics. We found that at higher temperatures the recovery ratio increased, because the crystalline melting could occur more thoroughly. At the same time, the stress required for programming decreased drastically, so even though the material could store stress more effectively, the recovery stress decreased significantly.

We showed that through self-reinforcement, we can increase the recovery stress of SMPs. By these same principles, shape memory SRPCs can be developed, which have lower density than conventional composites and aren't impeded in their biocompatibility or biodegradability by the presence of the reinforcing fibers; such properties will be advantageous in some biomedical, aerospace, or robotics applications.

CRediT authorship contribution statement

Balázs Tatár: Writing – original draft, Visualization, Validation, Investigation, Data curation. **Renáta Homlok:** Writing – review & editing, Resources, Investigation. **László Mészáros:** Writing – review & editing, Supervision, Resources, Methodology, Funding acquisition, Conceptualization.

Declaration of competing interest

The authors declare that they have no known competing financial interests or personal relationships that could have appeared to influence the work reported in this paper.

Acknowledgments

This work was supported by the National Research, Development and Innovation Office, Hungary (FK138501 and FK142540). Project no. TKP-6-6/PALY-2021 has been implemented with the support provided by the Ministry of Culture and Innovation of Hungary from the National Research, Development and Innovation Fund, financed under the TKP2021-NVA funding scheme. This research was funded by the National Research, Development and Innovation Fund of Hungary in the frame of GINOP_PLUSZ-2.1.1-21-2022-00041 project. The authors also extend their acknowledgment to the International Atomic Energy Agency (IAEA) for financial support under the umbrella of CRP (Coordinated Research Project/F23036/).

References

[1] B. Santhosh, et al., Shape Memory Materials, CRC Press, Boca Raton, 2018.
[2] P. Jyotishkumar, et al., Shape memory polymers. Blends and Composites Advances and Applications, Singapore: Springer, Singapore, 2019.
[3] D. Margoy, et al., Epoxy-based shape memory composite for space applications, Acta Astronaut. 178 (2021) 908–919.
[4] G. Guggenbiller, et al., 3D printing of green and renewable polymeric materials: toward greener additive manufacturing, ACS Appl. Polym. Mater. 5 (5) (2023) 3201–3229.
[5] K. Mirasadi, et al., Investigating the effect of ABS on the mechanical properties, morphology, printability, and 4D printing of PETG-ABS blends, Macromol. Mater. Eng. 309 (6) (2024) 2400038.
[6] D. Rahmatabadi, et al., 4D printing thermo-magneto-responsive PETG-Fe3O4 nanocomposites with enhanced shape memory effects, Appl. Mater. Today 40 (2024) 102361.
[7] M. Aberoumand, et al., Stress recovery and stress relaxation behaviors of PVC 4D printed by FDM technology for high-performance actuation applications, Sensor Actuator Phys. 361 (2023) 114572.
[8] Y.L. Xia, et al., A review of shape memory polymers and composites: mechanisms, materials, and applications, Adv. Mater. 33 (2021).
[9] M. Behl, J. Zotzmann, A. Lendlein, Shape-Memory Polymers, Germany: Springer, Berlin, Heidelberg, 2010.
[10] B. Tatár, L. Mészáros, Shape memory polymers: current state and future prospects, Express Polym. Lett. 17 (2023), 674-674.
[11] S. Ota, Current status of irradiated heat-shrinkable tubing in Japan, Radiat. Phys. Chem. 18 (1–2) (1981) 81–87.
[12] P. Jyotishkumar, et al., Shape memory polymers. Blends and Composites Advances and Applications, Springer, Singapore, 2019.
[13] M. Fejos, G. Romhany, J. Karger-Kocsis, Shape memory characteristics of woven glass fibre fabric reinforced epoxy composite in flexure, J. Reinforc. Plast. Compos. 31 (22) (2012) 1532–1537.
[14] S. Wang, et al., Ag/BN/EVA yarn artificial muscles with low drive voltage, high load capacity, and high Energy density, ACS Appl. Polym. Mater. 6 (17) (2024) 10951–10960.
[15] W. Baranowska, et al., Radiation and radical grafting compatibilization of polymers for improved bituminous binders—a review, Materials 17 (7) (2024) 1642.
[16] Y.K. Wang, et al., Short glass fiber reinforced radiation crosslinked shape memory SBS/LLDPE blends, J. Appl. Polym. Sci. 131 (17) (2014) 40691.
[17] T. Zaharescu, et al., Structural insights into LDPE/UHMWPE blends processed by γ-irradiation, Polymers 15 (3) (2023) 696.
[18] Y.K. Wang, et al., An investigation on shape memory behavior of glass fiber/SBS/LDPE composites, J. Polym. Res. 21 (8) (2014) 515.
[19] Y.K. Wang, et al., Thermomechanical and shape memory properties of SCF/SBS/LLDPE composites, Chin. J. Polym. Sci. 34 (11) (2016) 1354–1362.
[20] S. Rezanejad, M. Kokabi, Shape memory and mechanical properties of cross-linked polyethylene/clay nanocomposites, Eur. Polym. J. 43 (7) (2007) 2856–2865.
[21] L. Ma, et al., Effects of carbon black nanoparticles on two-way reversible shape memory in crosslinked polyethylene, Polymer 56 (2015) 490–497.
[22] R. Zhang, et al., Analysis of thermal-active bending and cyclic tensile shape memory mechanism of UHMWPE/CNT composite, Polym. Compos. 43 (12) (2022) 9089–9099.
[23] A. Kmetty, T. Barany, J. Karger-Kocsis, Self-reinforced polymeric materials: a review, Prog. Polym. Sci. 35 (10) (2010) 1288–1310.
[24] I. Nemes-Károly, G. Szebényi, Improving optical damage analysis of knee implants from an engineering perspective, Period. Polytech. - Mech. Eng. 67 (2) (2023) 151–160.
[25] Castres, et al., Static and dynamic behaviour of ultra high molecular weight polyethylene (UHMWPE) Tensylon® composite, Express Polym. Lett. 18 (2024) 1008–1022.
[26] Y.-F. Huang, et al., Mechanical properties and biocompatibility of melt processed, self-reinforced ultrahigh molecular weight polyethylene, Biomaterials 35 (25) (2014) 6687–6697.
[27] J. Wang, et al., Fabric insert injection molding for the preparation of ultra-high molecular weight polyethylene/high-density polyethylene two-component self-reinforced composites, Polymers (Basel) 14 (20) (2022).
[28] J.L.J. van Dingenen, High performance dyneema fibres in composites, Mater. Des. 10 (2) (1989) 101–104.
[29] L. Meszaros, et al., Novel, injection molded all-polyethylene composites for potential biomedical implant applications, J.Mater.Res.Technol.Jmr. amp.T 17 (2022) 743–755.
[30] C. Roiron, et al., Characterization of self-reinforced polyethylene recyclates according to different valorization strategies, J. Appl. Polym. Sci. 141 (32) (2024) e55822.
[31] M.S. Amer, S. Ganapathiraju, Effects of processing parameters on axial stiffness of self-reinforced polyethylene composites, J. Appl. Polym. Sci. 81 (5) (2001) 1136–1141.
[32] H. Liu, et al., Flexible, lightweight, high strength and high efficiently hierarchical Gd2O3/PE composites based on the UHMWPE fibers with self-reinforcing strategy for thermal neutron shielding, Compos. Sci. Technol. 251 (2024) 110549.
[33] J.-J. Park, et al., Improved processability for ultra-high molecular weight polyethylene/polyolefin elastomer composites: effect of ethylene vinyl acetate copolymer, Polym. Eng. Sci. 64 (7) (2024) 3203–3214.
[34] E. Statnik, et al., Formation mechanism of a self-reinforced UHMWPE-based composite material under high pressure, Mater. Lett. 382 (2025) 137900.

[35] B. Tatár, L. Mészáros, Shape memory effect in cross-linked polyethylene matrix composites: the effect of the type of reinforcing fiber, Polym. Bull. 81 (2023) 6311–6323.
[36] Y. Li, et al., High-performance fibrous artificial muscle based on reversible shape memory UHMWPE, J.Mater.Res.Technol.Jmr. amp.T 20 (2022) 7–17.
[37] A.V. Maksimkin, et al., Coiled artificial muscles based on UHMWPE with large muscle stroke, Mater. Today Commun. 21 (2019).
[38] A.V. Maksimkin, et al., Artificial muscles based on coiled UHMWPE fibers with shape memory effect, Express Polym. Lett. 12 (12) (2018) 1072–1080.
[39] A. Maksimkin, et al., Comparison of shape memory effect in UHMWPE for bulk and fiber state, J. Alloys Compd. 586 (2014) S214–S217.
[40] B. Wunderlich, Thermal Analysis, Academic Press, San Diego, 2012.
[41] L.H.J. Jeewantha, et al., Early research of shape memory polymer vascular stents, Express Polym. Lett. 16 (2022) 902–923.
[42] M.M.R. Khan, M.E. Hossain, R. Jayaraman, Effect of fiber surface treatments on the strength of bonding between dyneema® fiber and HDPE matrix, Compos. Interfaces 27 (12) (2020) 1061–1083.
[43] W. Miao, et al., High-density polyethylene crystals with double melting peaks induced by ultra-high-molecular-weight polyethylene fibre, R. Soc. Open Sci. 5 (7) (2018) 180394.
[44] A.J. Peacock, Handbook of Polyethylene : Structures, Properties, and Applications, Dekker, New York, 2000.